



Diachronic Study of Halophyte vegetation in the Constantine highlands (Sebkhat Ezzemoul and Chott Tinsilt) Northeastern of Algeria

Asma Boudehane¹, Hassen Benmessaoud², Ayache Laabassi^{1*}, Azzedine Fercha³

¹Department of Ecological and Environmental Sciences, Faculty of Natural and Life Sciences, University of Batna 2, Algeria

²Institute of Veterinary Sciences and Agricultural Sciences, University of Batna 01, Algeria

³Department of Agronomy, Abbes Laghrour University, Khenchela, Algeria

*Corresponding Author: a.laabassi@univ-batna2.dz

ARTICLE INFO

Article History:

Received: May 18, 2025

Accepted: July 19, 2025

Online: July 27, 2025

Keywords:

Halophytes,
Geomatic,
Spatio-temporal,
Sebkhat Ezzemoul,
Chott Tinsilt

ABSTRACT

This research focused on monitoring the spatial and temporal dynamics of halophyte vegetation in Sebkhat Ezzemoul (6,765 ha) and Chott Tinsilt (2,154 ha), which are part of the wetland system in the high plateaus of Constantine, northeastern Algeria. Conducted within a semi-arid climate, the study employed geomatics tools to analyze changes over time. A 30-year diachronic study (1987–2017) was carried out using LANDSAT satellite imagery from the years 1987, 2000, and 2017. The findings indicate that variations in halophyte species are primarily influenced by key environmental factors, including agricultural practices and overgrazing.

INTRODUCTION

The wetland complex of the high plateaus in eastern Algeria (the Constantinois) comprises approximately twenty natural wetlands (Chotts, Sebkhes, and Garaets) scattered across the provinces of Oum El Bouaghi, Khenchela, and Batna. These wetlands stretch over a distance of 300km and cover an area of 55,000 ha (Amri *et al.*, 2019). Sebkhet Ezzemoul is located to the east of Chott Tinsilt, and together, these two wetlands encompass an area of 8,919 ha. They are temporary wetlands that fill only during significant rainfall events in the winter season. These plains cover an area of 4,600 ha (Boulekhssaim *et al.*, 2006; Messai *et al.*, 2006; Aliat *et al.*, 2016; Amri *et al.*, 2019).

The approach adopted in this study is purely cartographic, enabling the compilation of general information about the study site (exposure, slope, coverage, geographical coordinates, altitude, etc.) and its analysis through specialized software to produce NDVI (Normalized Difference Vegetation Index) and change maps.

To achieve this, we aimed to answer the following two questions:

1. What is the wetland's evolution over time?
2. What are the main factors influencing this evolution?

MATERIALS AND METHODS

Study area

Sebkhet Ezzemoul and Chott Tinsilt are located in northeastern Algeria (35°53'14"N, 6°28'44"E and 35°53'14"N, 06°30'20"E, respectively) in the province of Oum El Bouaghi (Fig. 1). They are characterized by a semi-arid to arid Mediterranean climate, with an average annual rainfall of about 300mm and average temperatures ranging from approximately 3 to 37°C. Sebkhet Ezzemoul covers an area of 6,765 ha, with a maximum estimated depth of 0.40m (Moali & Remichi, 2009). In contrast, the floodable area of Chott Tinsilt is approximately 1,000 ha, while the entire site, including its surroundings, spans around 3,600 ha (Saheb, 2003). Both wetlands are listed under the Ramsar Convention.

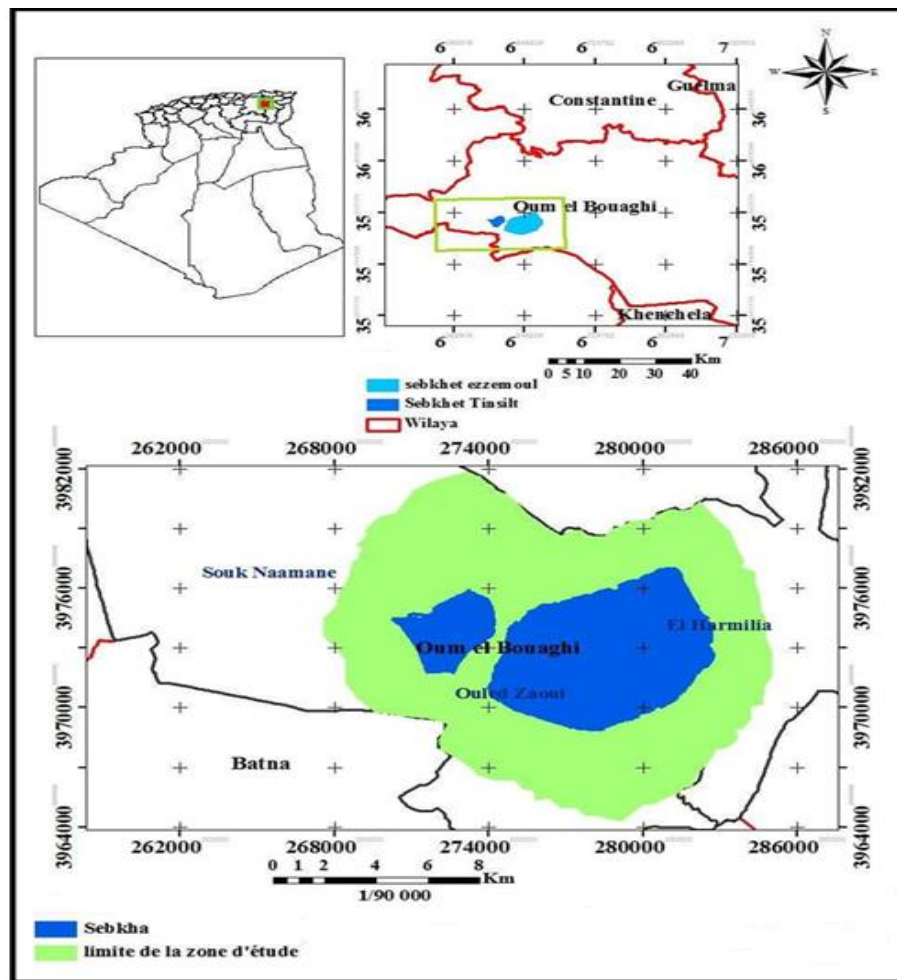


Fig. 1. Map of the study site

Materials and methods

The setup primarily includes a Garmin GPS receiver (Model GPS map 60Cx) for georeferencing the study site and a digital camera for capturing images.

Data used**Cards**

Topographic maps at a scale of 1:50,000 (Geodetic System North Sahara 1959, Clarke 1880 Ellipsoid, UTM Projection Zone 32 North) were used in digital format to delineate the study area's boundaries and analyze the terrain. The specific sheets used include Batna East (SHEET NI-32-XIX-3), Ain Fakroun West (SHEET NI-32-XIX-2), Chemora West (SHEET NI-32-XIX-4), and Souk Naamane East (SHEET NI-32-XIX-1). Additionally, thematic maps of land use and lithology for the Batna province, produced by the National Office for Rural Development Studies (NORDS), were utilized.

Maps and satellite imagery

This study employed satellite images from LANDSAT 5 TM (1987), LANDSAT 7 ETM+ (2002), and LANDSAT 8 LDCM (2017) to perform various image processing techniques such as false color composition and calculation of the Normalized Difference Vegetation Index (NDVI). A 30-meter resolution SRTM Digital Terrain Model (DTM) of Eastern Algeria was used to generate slope and aspect (exposure) maps of the study area. For image processing and analysis, Global Mapper 13, ArcGIS 9.3, and ENVI 5.0 software were used.

Mapping approach

A central goal of this study was to monitor changes in halophyte vegetation in Sebkhet Ezzemoul and Chott Tinsilt over a 30-year period (1987–2017). To achieve this, remote sensing and GIS techniques were employed to produce maps that visualize vegetation dynamics over time.

Acquisition of satellite images

LANDSAT imagery was selected for this study for two main reasons:

1. LANDSAT is the oldest Earth observation program, offering a long-term archive of over 30 years of imagery.
2. LANDSAT data is freely available through the United States Geological Survey (USGS) platform, a U.S. government agency focused on Earth sciences.

Selection of image dates

In diachronic vegetation studies, careful selection of image dates is crucial due to seasonal variability in field conditions. A major challenge is distinguishing natural vegetation—particularly herbaceous species—from cultivated land. Since vegetation monitoring relies on photosynthetic activity, imagery was selected from the spring season, when natural vegetation is most active.

Applying a mask and false color composition

A false color composite was applied using band combinations 4-3-2 for LANDSAT 5 and 7, and 5-4-3 for LANDSAT 8. These bands correspond to near-infrared, red, and green wavelengths and are displayed as red, green, and blue on screen, respectively. This composition is effective for vegetation analysis due to the strong reflectance of healthy vegetation in the near-infrared range. On such images, high-activity vegetation appears bright red, water appears almost black due to high absorption, and bare or mineral surfaces show up in blue to white shades.

Calculation of NDVI and change detection

As noted earlier, this study aimed to monitor the spatial and temporal evolution of halophyte vegetation in Sebkhet Ezzemoul and Chott Tinsilt from 1987 to 2017. NDVI values were calculated from satellite imagery for three dates: March 28, 1987; April 24, 2000; and April 10, 2017. These dates correspond to the peak vegetation period in spring, which enhances comparability. By comparing NDVI maps from each date, vegetation cover changes in the study area were detected and visualized in a change map.

The methodological steps of this approach are summarized in Fig. (2).

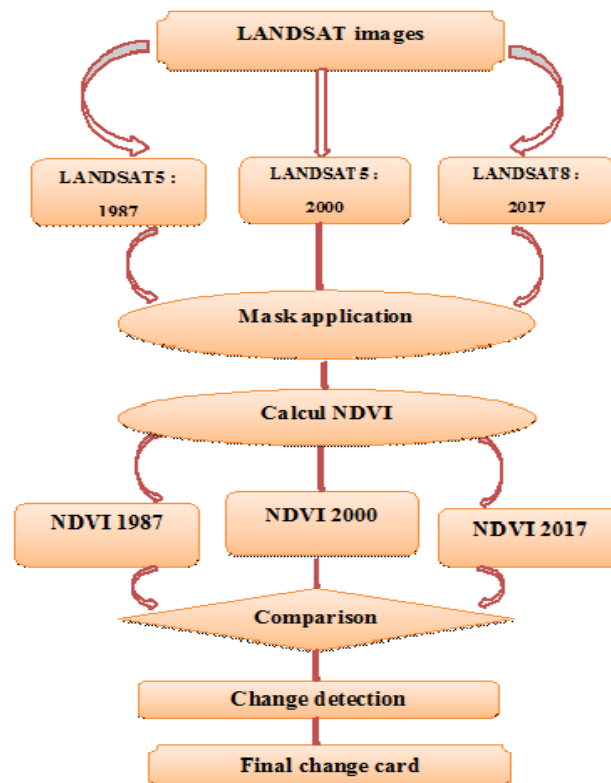


Fig. 2. Methodological flowchart

RESULTS

Cartographic results

Using geomatics tools makes it possible to produce multi-date NDVI maps and change maps in order to better evaluate the objective of our work.

NDVI results

The NDVI results of this study show an increasing gradient of plant activity with values ranging between -1 and +1; values close to -1 indicate the decrease in vegetation, while those close to +1 indicate that the vegetation is growing well and in good health. The first method to specify the vegetation in an area is the average of NDVI values within the area. This solution supplies information about vegetation (Alatorre *et al.*, 2013; Zaitunah *et al.*, 2018; Csete *et al.*, 2021; Pushpanjali *et al.*, 2021).

Because vegetation cover is highly dynamic—affected by both climate change and human activities—the NDVI values are often found to vary significantly across different case studies. Therefore, it is essential not only to detect changes but also to evaluate the extent of change in plant cover (Peng *et al.*, 2012).

Each color displayed on the map indicates a different level of land cover change. The color gradient is interpreted as follows:

- **Black to dark orange:** bare ground
- **Light brown:** sparsely vegetated areas
- **Orange to yellow:** moderately dense vegetation
- **Bright yellow:** dense vegetation

The NDVI results appeared as follows:

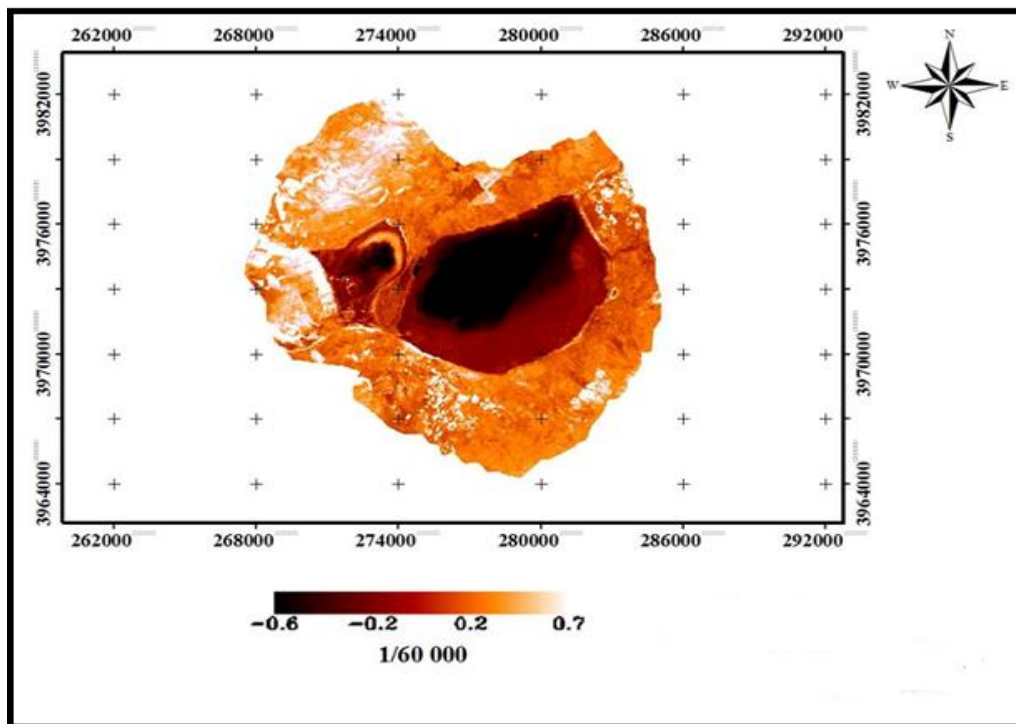


Fig. 3. NDVI map of the study site (1987)

According to the 1987 NDVI map (Fig. 3), values can be categorized into three main classes:

- **Bare soil:** NDVI values ranging from -0.6 to -0.2
- **Medium dense vegetation:** NDVI values from -0.2 to 0.2
- **Dense vegetation:** NDVI values between 0.2 and 0.7

A visual interpretation of the 1987 NDVI map indicates that vegetation during this period was relatively dense and primarily concentrated around Sebkhet Ezzemoul and Chott Tinsilt.

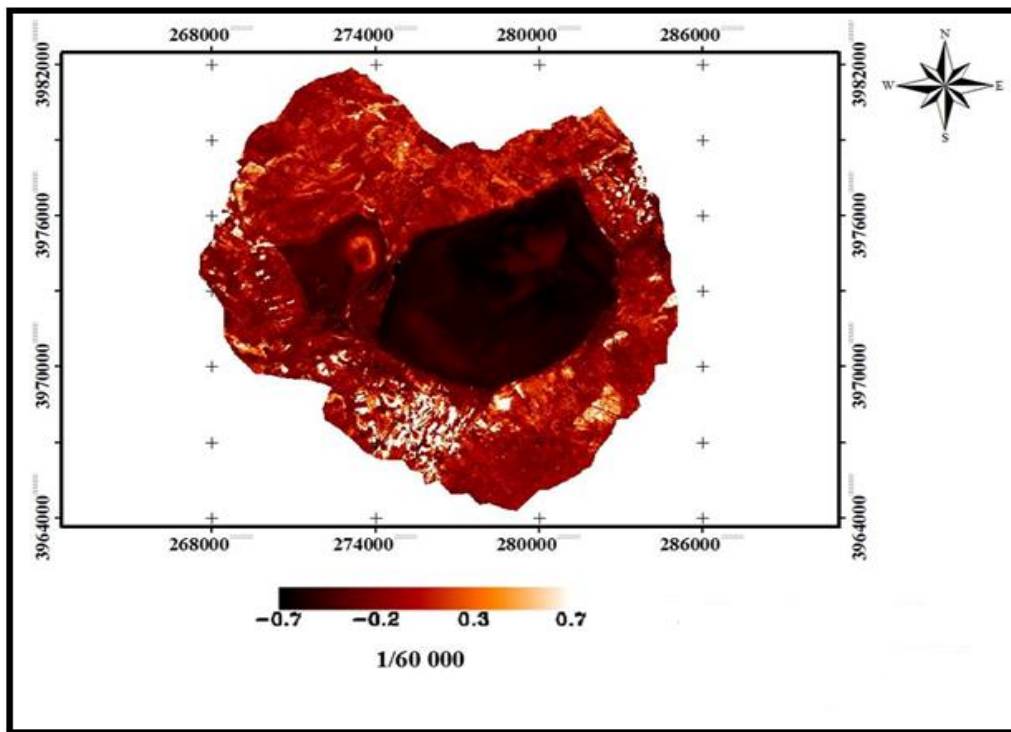


Fig. 4. NDVI map of the study site (2000)

Fig. (4) summarizes the NDVI map results for the study site in the year 2000. The NDVI values fall into the following categories:

- **-0.7 to -0.2:** bare soil
- **-0.2 to 0.3:** medium dense vegetation
- **0.3 to 0.7:** dense vegetation
- **>0.7:** agricultural vegetation

Visual interpretation of this map indicates that dense vegetation is primarily concentrated to the north of Sebkhet Ezzemoul and Chott Tinsilt. Moderately dense vegetation surrounds the site, while bare ground appears mainly in the center and along the northern and eastern edges of the study area. Additionally, a noticeable reduction in

vegetated areas is observed in the northern region, accompanied by an increase in bare soil. This shift reflects a clear trend of vegetation regression.

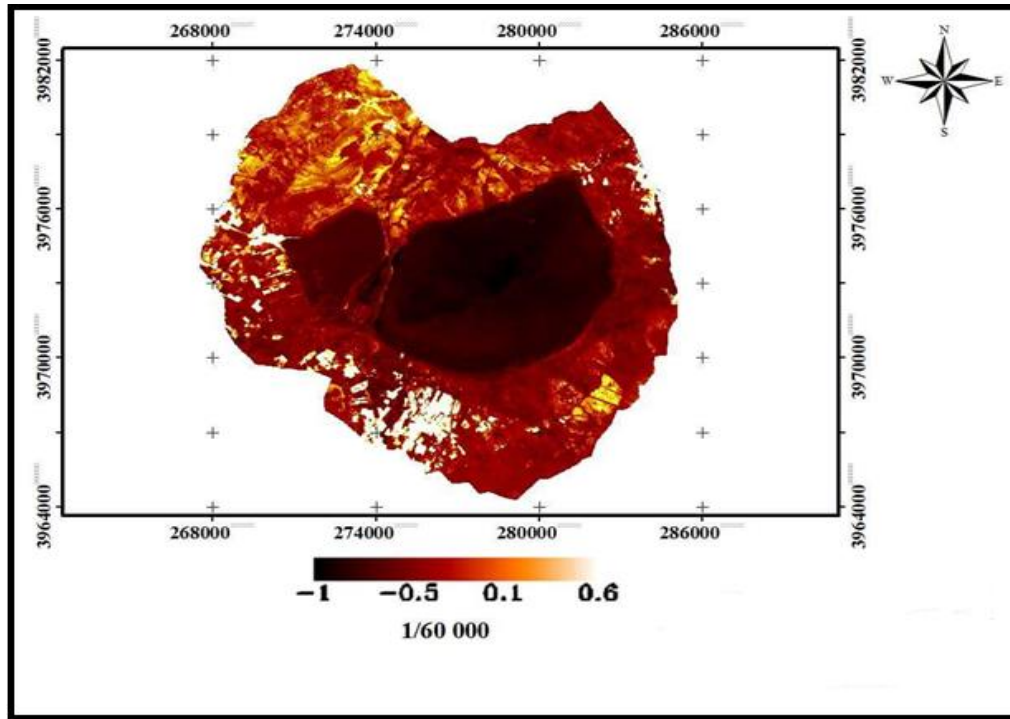


Fig. 5. NDVI map of the study site (2017)

In the NDVI image from 2017 (Fig. 5), the NDVI values are categorized as follows:

- **-1 to -0.5:** bare ground
- **-0.5 to 0.1:** moderately dense vegetation
- **0.1 to 0.6:** dense vegetation
- **> 0.6:** agricultural vegetation

Visual interpretation of the 2017 NDVI map shows that dense vegetation is primarily located in the northern and eastern parts of the study area. Moderately dense vegetation and bare soil remain largely distributed in the same areas as in 2000. Agricultural vegetation is dominant in the southern and western parts, while bare soil is concentrated in the center and along the eastern edges of Sebkhet Ezzemoul and Chott Tinsilt.

It is important to note that the maximum NDVI value (NDVI max = 0.7) was recorded in 1987 and remained the same in 2000. However, in 2017, this value decreased to 0.6. This decline in NDVI can be attributed to the degradation of halophyte vegetation in the study area.

Change map results

The change detection analysis covers the same period. The trend between 1987 and 2000 (Fig. 6) clearly indicates a regression of vegetation, particularly in the western part of the site, and similarly in the east. In the central region, the vegetation regression is less significant. Vegetation progression is minimal, especially in the southern part of the study area, although there is a noticeable improvement in the eastern region.

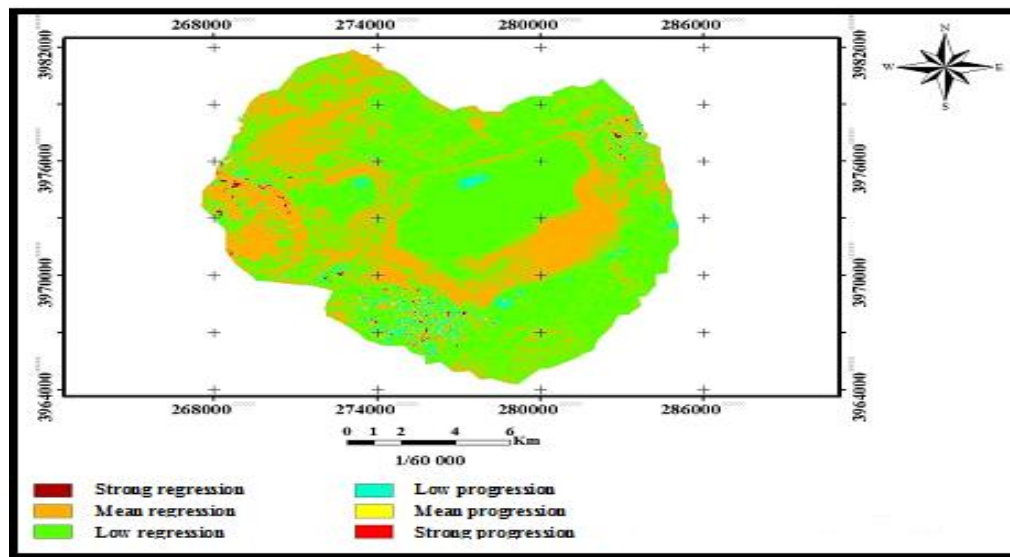


Fig. 6. Change detection map of the study area (1987-2000)

As shown in Fig. (7), the analysis reveals that the majority of the surface area experienced slight regression, covering approximately 13,489.72 ha. Moderate regression is observed around the perimeter of Sebkheth Ezzemoul, with a relatively significant area of 6,651.05 ha transitioning to bare soil. Strong regression is concentrated in the western and southern parts of the study area, where 46.55 ha—previously covered by halophyte vegetation—have been lost. In contrast, the total area showing vegetation progression is relatively small and appears as isolated patches on the map.

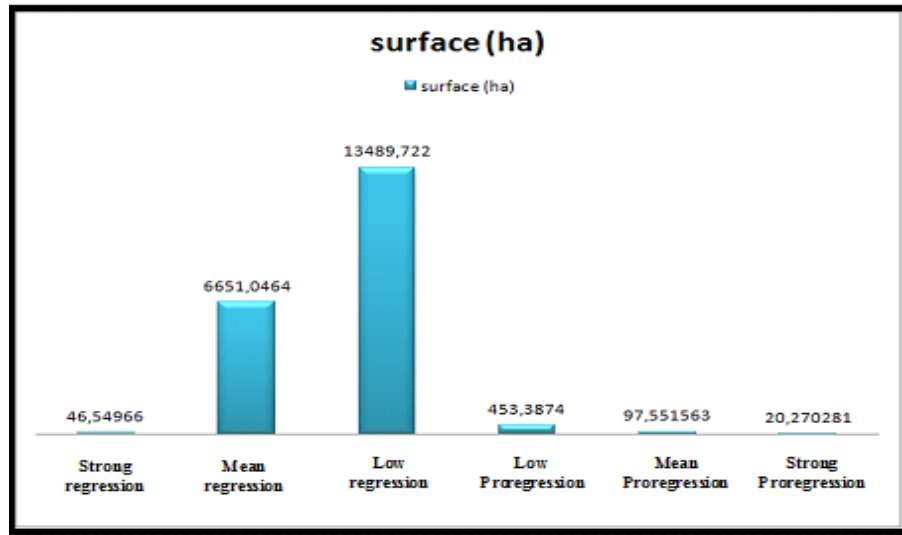


Fig. 7. Change detection diagram of the study area (1987-2000)

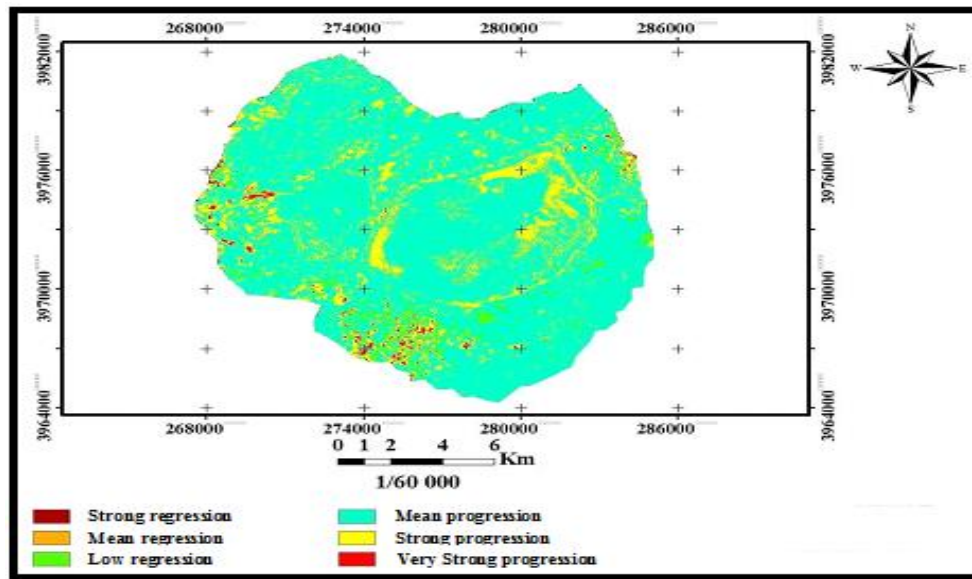


Fig. 8. Change detection map of the study area (2000-2017)

Analysis of the results presented in Fig. (8) establishes a relationship between the state of vegetation and the type of detected changes. The regression observed between 2000 and 2017—indicating vegetation deterioration—is relatively moderate, with areas of strong progression located in the central part of the map. This progression reflects an overall increase in vegetation cover across much of the study area.

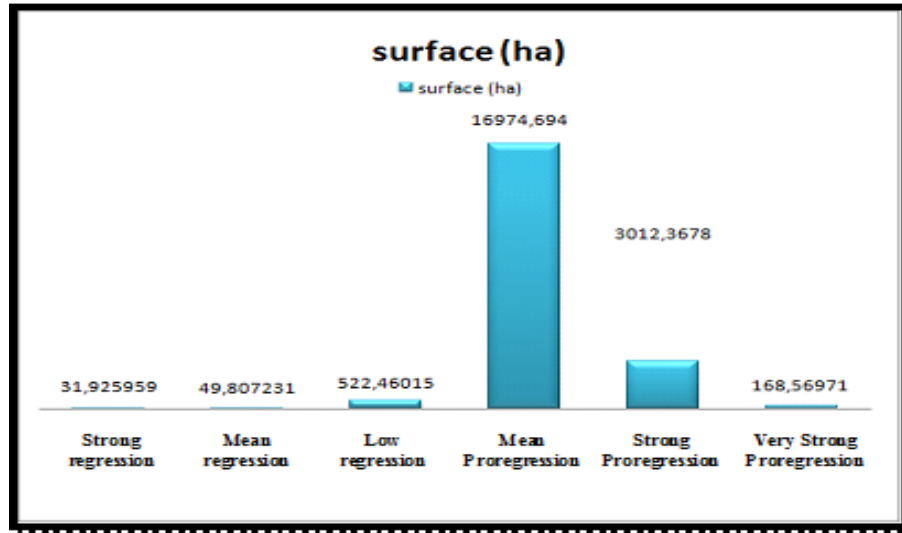


Fig. 9. Change detection diagram of the study area (2000-2017)

As shown in Fig. (9), over a total area of 6,765 ha, the regression recorded over a 23-year period amounts to 604.19 ha, indicating slight degradation—primarily due to the reduction of halophyte vegetation. During the same period, a significantly larger regression area of 20,155.63 ha was recorded, primarily located in the central part of the Sebkhet.

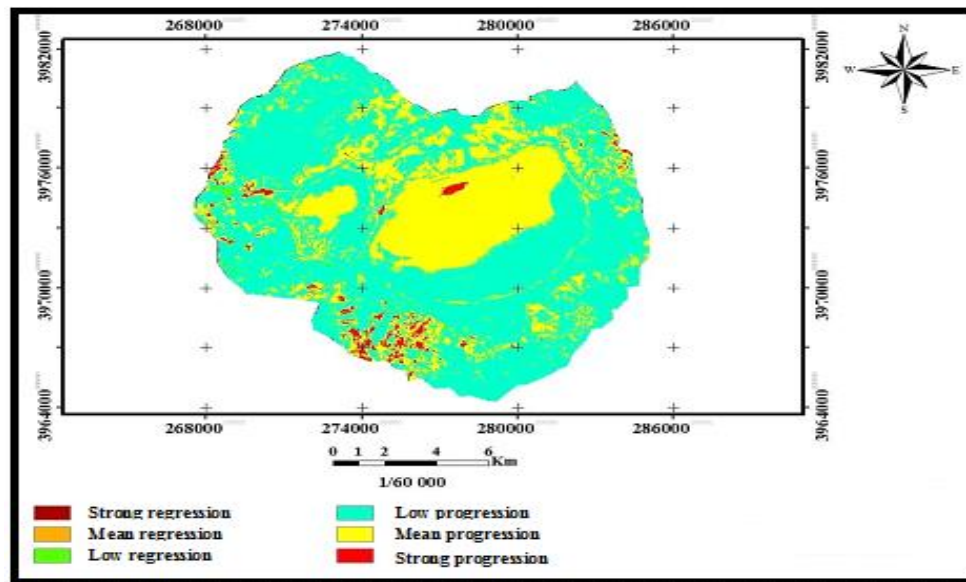


Fig. 10. Change detection map of the study area (1987-2017)

Between 1987 and 2017, vegetation progression within the Sebkhet is particularly noticeable and pronounced, especially in the central part of the map, where it covers a significant area. Strong progression is also evident in the eastern, western, and particularly southern sectors, largely attributed to agricultural activities. Conversely, the map reveals slight regression, represented by moderately sized patches scattered

throughout various parts of the study area (Fig. 10). Despite the overall trend of progression, a notable decline in halophyte vegetation is observed in some areas, indicating localized but significant vegetation degradation.

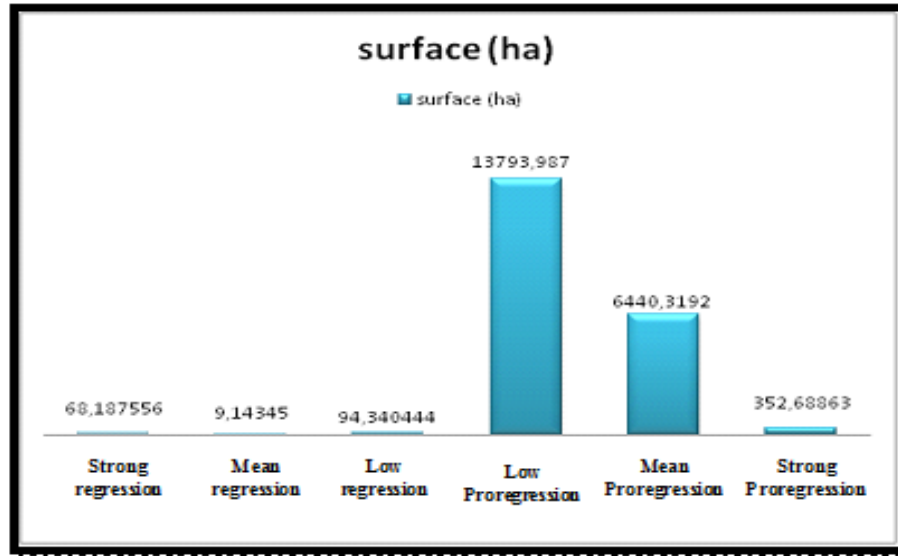


Fig. 11. Change detection map of the study area (1987-2017)

Fig. (11) also shows a significant progression of vegetation, covering an area of 20,586.99 ha. This expansion reflects a decrease in the water level of the Sebkhet and affects nearly the entire study area. In contrast, the regressed areas are limited, representing only 171.67 ha.

DISCUSSION

In this study, the focus was on processing multi-temporal remote sensing data to track the evolution of halophyte vegetation in Sebkhet Ezzemoul and Chott Tinsilt. By comparing NDVI values across three different years, and based on the analysis results, four primary land cover types were identified:

1. Sebkhets
2. Agricultural areas
3. Halophyte vegetation
4. Bare soils

Over the three reference dates, the change detection maps show a marked regression in vegetation cover (Van Der Schriek & Giannakopoulos, 2017; Law *et al.*, 2018; Scordo *et al.*, 2018; Woolway *et al.*, 2019; Pushpanjali *et al.*, 2021), while agricultural areas significantly expanded (Zender *et al.*, 2004; Rodríguez *et al.*, 2012). This expansion of agriculture has come at the cost of halophyte vegetation, whose coverage has steadily declined.

These changes suggest that climate—particularly precipitation—plays a major role in shaping vegetation dynamics under water-limited conditions (Chen *et al.*, 2018; Negesse *et al.*, 2024). In arid regions, where the average annual rainfall is around 300mm, plant growth is more sensitive to rainfall than temperature. The decline in vegetation is therefore primarily associated with persistent water stress (Bao *et al.*, 2014; Chen *et al.*, 2018; Wang *et al.*, 2019). These findings are consistent with previous studies (You *et al.*, 2019; Setti *et al.*, 2023).

In addition to climatic factors, human activities—especially agricultural expansion and overgrazing—are major contributors to the regression of halophyte vegetation (Vitousek *et al.*, 1997). Combined with natural stressors, anthropogenic pressures further intensify ecosystem degradation (Liu *et al.*, 2018; Chen *et al.*, 2019; Xu *et al.*, 2021). The conversion of Sebkhetts and Chotts into cereal cropland, urbanization, and increased livestock numbers—particularly under nomadic pastoralism—have all contributed to vegetation decline. Livestock farming remains a dominant livelihood in rural areas (Vitousek *et al.*, 1997; Wang *et al.*, 2019), and overgrazing has accelerated grassland degradation (Verbrugge *et al.*, 2022).

Simultaneously, agricultural practices are becoming more intensive, expanding into fragile ecosystems. This trend underscores the need for sustainable land management strategies. In this context, geomatics and remote sensing technologies provide efficient tools for studying ecological transformations (You *et al.*, 2016; Liu *et al.*, 2018; Peng *et al.*, 2019; Yuan *et al.*, 2022). These tools help identify changes and support decision-making for conservation and land use planning.

CONCLUSION

This study demonstrates that both climate variability and human activities are the main drivers of plant cover distribution in the Sebkhet Ezzemoul and Chott Tinsilt region. In particular, anthropogenic pressures—such as agricultural expansion and overgrazing—pose a serious threat to the regeneration of halophyte vegetation in the medium term.

The results reveal a clear pattern of change over the study period (1987–2017), driven primarily by increasing agricultural activity. This has led to the degradation of halophyte-dominated ecosystems and a reorganization of land cover across the region.

The use of cartographic approaches and geomatics has proven to be an effective methodology for analyzing ecological dynamics. These tools can support the reorganization of research efforts and guide a comprehensive, participatory conservation management strategy.

Finally, the implementation of conservation programs in vulnerable areas is essential to preserving the region's biodiversity. Targeted interventions, informed by remote sensing and field-based data, could help safeguard these unique ecosystems under the current and future pressures of climate change and human impact.

REFERENCES

- Alatorre, L. C.; Sánchez-Carrillo, S.; Miramontes-Beltrán, S.; Medina, R. J.; Torres-Olave, M. E. and Bravo, L. C. Uc. M. (2016). Temporal changes of NDVI for qualitative environmental assessment of mangroves: Shrimp farming impact on the health decline of the arid mangroves in the Gulf of California (1990–2010). *J. Arid. Environ.*, 125, 98–109. <https://doi.org/10.1016/j.jaridenv.2015.10.010>
- Aliat, T.; Kaabeche, M.; Khomri, H.; Nouri, L.; Neffar, S. and Chenchouni H. (2016). A pedological characterisation of some inland wetlands and Ramsar sites in Algeria. *Land Degrad. Dev.*, 27(3), 693–705. <https://doi.org/10.1002/ldr.2467>
- Amri, C.; Neffar, S.; Ouchtati, N. and Chenchouni, H. (2019). Spatiotemporal patterns of ground beetle diversity (Coleoptera: Carabidae) in a Ramsar wetland (Chott Tinsilt) of Algeria. *Turk J Zool.*, 43, 502–515. <https://doi.org/10.3906/zoo-1904-19>
- Bao, G. Z.; Qin, Y.; Bao, Y.; Zhou, W.Li. and Sanjjav, A. (2014). NDVI-Based Long-Term Vegetation Dynamics and Its Response to Climatic Change in the Mongolian Plateau. *Remote Sens.*, 6, 8337–8358. <https://doi.org/10.3390/rs6098337>
- Boulekhssaim, M.; Houhamdi, M. and Samraoui, B. (2006). Status and diurnal behaviour of the Shelduck Tadorna tadorna in the Hauts Plateaux, Northeast Algeria. *Wildfowl.*, 56, 65–78. <https://wildfowl.wwt.org.uk/index.php/wildfowl/article/view/1184>
- Chen, C.; He, B.; Guo, L.; Zhang, Y.; Xie, X. and Chen, Z. (2018). Identifying critical climate periods for vegetation growth in the northern hemisphere. *J Geophys Res Biogeosci.*, 123, 2541–2552. <https://doi.org/10.1029/2018JG004443>
- Chen, L. D.; Hu, W.; Li, D. Q.; Cheng, D. M. and Zhong, A.W. (2019). Prediction of suitable distribution areas of the endangered plant wild Nelumbo nucifera Gaertn.in China. *Plant Sci.*, 37(06), 731–740. <https://www.cabidigitallibrary.org/doi/full/10.5555/20203151699>
- Csete, Á. K., Kolcsár, R. A. and Gulyás, Á. (2021). Rainwater harvesting potential and vegetation irrigation assessment derived from building databased hydrological modelling through the case study of Szeged. *Carpathian J. Earth Environ. Sci.*, 16 (2), 469–482. <https://doi.org/10.26471/cjees/2021/016/192>
- Cui, L.; Qiu, Y.; Fei, T.; Liu, Y. and Wu, G. (2013). Using remotely sensed suspended sediment concentration variation to improve management of Poyang Lake, China. *Lake Reserv. Manag.*, 29 (1), 47–60. <https://doi.org/10.1080/10402381.2013.768733>
- Law, A. C.; Nobajas, A. and Sangonzalo, R. (2018). Heterogeneous changes in the surface area of lakes in the Kangerlussuaq area of southwestern Greenland

- between 1995 and 2017. *Arct. Antarct. Alp. Res.*, 50(1), <https://doi.org/10.1080/15230430.2018.1487744>
- Liu, G.; Liu, H. and Yin, Y.** (2013). Global patterns of NDVI-indicated vegetation extremes and their sensitivity to climate extremes. *Environ. Res. Lett.*, 8 (2), 025009. <https://doi.org/10.1088/1748-9326/8/2/025009>
- Liu, H.; Zhang, M.; Lin, Z. and Xu, X.** (2018). Spatial heterogeneity of the relationship between vegetation dynamics and climate change and their driving forces at multiple time scales in Southwest China. *Agric. For. Meteorol.*, 256, 10–21. <https://doi.org/10.1016/j.agrformet.2018.02.015>
- Messai, N.; Aouati, A. and Berchi, S.** (2016). Impact of the Surface Water Physicochemical Parameters on Culicidae (Diptera: Nematocera) of Lakeside Ecosystem “Sebkhet Ezzemoul” (Oum El Bouaghi–Algeria). *J Entomol Zool Stud.*, 4, 391–8. <https://www.entomoljournal.com/archives/2016/vol4issue3/PartF/4-3-61-107.pdf>
- Moali, A. and Remichi, Z.** (2009). Sebkhet Ezzemoul (Wilaya d’Oum El Bouaghi). *Fiche descriptive sur les zones humides Ramsar* (FDR). 12p.
- Negesse, M. D.; Hisheb, S. and Getahun, K.** (2024). LULC dynamics and the effects of urban green spaces in cooling and mitigating microclimate change and urban heat island effects: a case study in Addis Ababa City, Ethiopia. *J. Water Clim. Change*, 15 (7), 3033–3055. <https://doi.org/10.2166/wcc.2024.662>
- Peng, J.; Liu, Z. H.; Liu, Y. H.; Wu, J. S. and Han, Y. A.** (2012). Trend analysis of vegetation dynamics in Qinghai-Tibet Plateau using Hurst exponent. *Ecol. Indic.*, 14(1), 28–39. <https://doi.org/10.1016/j.ecolind.2011.08.011>
- Peng, W.; Kuang, T. and Tao, S.** (2019). Quantifying influences of natural factors on vegetation NDVI changes based on geographical detector in Sichuan, western China. *J. Clean. Prod.*, 233, 353–367. <https://doi.org/10.1016/j.jclepro.2019.05.355>
- Pushpanjali, S.; Josily, C. A.; Rama, K.; Raju, B. and Karthikeyan, K.** (2021). Spatial estimation and climate projected change of covermanagement factor in semi-arid region of India. *Indian J. Agric. Sci.*, 4, 521–525. <https://doi.org/10.56093/ijas.v91i4.112631>
- Rodríguez, N.; Armenteras, D. and Retana, J.** (2013). Effectiveness of Protected Areas in the Colombian Andes: Deforestation, Fire and Land-Use Changes. *Reg. Environ. Change.*, 13(2), 423–435. <https://link.springer.com/article/10.1007/s10113-012-0356-8>
- Saheb, M.** (2003). Cartographie et rôle de la végétation dans le maintien de l’avifaune aquatique des sebkhas de Guellif et de Boucif (Oum-El-Bouaghi). Thèse de Magister en Ecologie et Environnement. Centre Universitaire d’Oum El-Bouaghi, 59p.

- Setti, S.; Yumnam, K.; Rathinasamy, M. and Agarwal, A.** (2023). Assessment of satellite precipitation products at different time scales over a cyclone prone coastal river basin in India. *J Water Clim Chang.*, 14 (1), 38–65. <https://doi.org/10.2166/wcc.2022.166>
- Scordo, F.; Bohn, V. Y.; Piccolo, M. C. and Perillo, G. M. E.** (2018). Mapping and monitoring lakes intra-annual variability in semi-arid regions: a case of study in Patagonian Plains (Argentina). *Water*, 1, 889. <https://doi.org/10.3390/w10070889>.
- Van der Schriek, T. and Giannakopoulos, C.** (2017). Determining the causes for the dramatic recent fall of Lake Prespa (southwest Balkans). *Hydrol. Sci. J.*, 62 (7), 1131–1148. <https://doi.org/10.1080/02626667.2017.1309042>
- Verbrugge, L.; Bjarnason, G.; Fagerholm, N.; Magnussen, E.; Mortensen, L.; Olsen, E.; Plieninger, T.; Raymond, C. and Olafsson, A.** (2022). Navigating overgrazing and cultural values through narratives and participatory mapping: a socio-cultural analysis of sheep grazing in the Faroe Islands. *Ecosyst. People*, 18, 289–302. <https://doi.org/10.1080/26395916.2022.2067242>
- Vitousek, P. M.; Mooney, H. A.; Lubchenco, J. and Melillo, J. M.** (1997). Human domination of Earth's ecosystems. *Science.*, 277, 494–499. <https://doi.org/10.1126/science.277.5325.494>
- Wang, G.; Wang, P.; Wang, T. Y.; Zhang, Y. C.; Yu, J. J.; Ma, N.; Frolova, N. L. and Liu, C. M.** (2019). Contrasting changes in vegetation growth due to different climate forcings over the last three decades in the Selenga-Baikal Basin. *Remote Sens.*, 11, 1–17. <https://doi.org/10.3390/rs11040426>
- Woolway, R. I.; Weyhenmeyer, G. A.; Schmid, M.; Dokulil, M. T.; de Eyto, E. and Maberly, S. C.** (2019). Substantial increase in minimum lake surface temperatures under climate change. *Clim. Change*, 155(1), 81–94. <https://doi.org/10.1007/s10584-019-02465-y>.
- Xu, X. J.; Liu, H. Y.; Jiao, F. S.; Gong, H. B. and Lin, Z. S.** (2021). Nonlinear relationship of greening and shifts from greening to browning in vegetation with nature and human factors along the Silk Road Economic Belt. *Sci Total Environ.*, 766, 142553. <https://doi.org/10.1016/j.scitotenv.2020.142553>
- You, G.; Arain, M. A.; Wang, S.; McKenzie, S.; Zou, C.; Wang, Z.; Li, H.; Liu, B.; Zhang, X.; Gu, Y. and Gao, J.** (2019). The spatial-temporal distributions of controlling factors on vegetation growth in Tibet Autonomous Region, Southwestern China. *China. Environ. Res. Commun.*, 1, 1–12. <https://doi.org/10.1088/2515-7620/ab3d87>.
- You, N.; Meng, J. and Sun, M.** (2019). Spatio-temporal change of NDVI and its relationship with climate in the upper and middle reaches of Heihe River Basin from 2000 to 2015. *Acta Sci. Natur. Univ. Pekinensis.*, 55, 171–181. <https://doi.org/10.13209/j.0479-8023.2018.075>.

- Yuan, L.; Chen, X.; Wang, X.; Xiong, Z. and Song, C.** (2019). Spatial associations between NDVI and environmental factors in the Heihe River Basin. *J. Geogr. Sci.*, 29 (9), 1548–1564. <https://doi.org/10.1007/s11442-019-1676-0>
- Zaitunah, A.; Samsuri, S.; Ahmad, A. and Safitri, R.** (2018). Normalized difference vegetation index (ndvi) analysis for land cover types using landsat 8 oli in besitang watershed, Indonesia. IOP Conf. Ser. *Earth and Environmental Science.*, p126.
- Zender, C. S.; Miller, R. L. and Tegen, I.** (2004). Quantifying mineral dust mass budgets: Terminology, constraints, and current estimates. *Eos Transactions AGU.*, 85, 509–512. <https://doi.org/10.1029/2004EO4800>